



**HAL**  
open science

# A new experimental setup for high-throughput controlled non-photochemical laser-induced nucleation Application to glycine crystallization

Bertrand Clair, Aziza Ikni, Wenjing Li, Philippe Scoufflaire, V. Quemener,  
Anne Spasojevic - de Biré

## ► To cite this version:

Bertrand Clair, Aziza Ikni, Wenjing Li, Philippe Scoufflaire, V. Quemener, et al.. A new experimental setup for high-throughput controlled non-photochemical laser-induced nucleation Application to glycine crystallization. *Journal of Applied Crystallography*, 2014, 47 (4), pp.1252-1260. 10.1107/S160057671401098X . hal-02296127

**HAL Id: hal-02296127**

**<https://hal.science/hal-02296127v1>**

Submitted on 24 Sep 2020

**HAL** is a multi-disciplinary open access archive for the deposit and dissemination of scientific research documents, whether they are published or not. The documents may come from teaching and research institutions in France or abroad, or from public or private research centers.

L'archive ouverte pluridisciplinaire **HAL**, est destinée au dépôt et à la diffusion de documents scientifiques de niveau recherche, publiés ou non, émanant des établissements d'enseignement et de recherche français ou étrangers, des laboratoires publics ou privés.

# A new experimental setup for a high throughput controlled Non-Photochemical LASER-Induced Nucleation (NPLIN). Application to Glycine crystallization

Bertrand Clair<sup>1,2</sup>, Aziza Ikni<sup>1,2</sup>, Wenjing Li<sup>1,2</sup>, Philippe Scoufnaire<sup>1,3</sup>, Vincent Quemener<sup>4</sup>, Anne Spasojević-de Biré<sup>1,2\*</sup>

1 Ecole Centrale Paris, Grande Voie des Vignes, 92290 Châtenay-Malabry, France

2 CNRS, UMR 8580, Laboratoire "Structures Propriétés et Modélisation des Solides", Grande Voie des Vignes, 92295 Châtenay-Malabry, France

3 CNRS, UPR 288, Laboratoire d'Energétique Moléculaire et Macroscopique, Combustion (EM2C), Grande Voie des Vignes, 92290 Châtenay-Malabry, France

4 ARCALE, 1 rue des Pénitents Blancs, BP 71028, 31010 Toulouse CEDEX 6

**Synopsis** A new experimental setup for a high throughput controlled Non-Photochemical LASER-Induced Nucleation (NPLIN) has been designed. Nucleation efficiency of Glycine as a function of the supersaturation of the solution used and the LASER beam energy density has been established on a large number of samples.

**Abstract** Non-Photochemical LASER-Induced Nucleation (NPLIN) is a growing field of studies since 1996, with more than 40 compounds including organic, inorganic and proteins probed under various conditions (solvents, LASER types, LASER beams ...). The potential advantages using this technique are huge, in particular polymorphic control. To realize these benefits, the objective is a carefully designed experimental setup and highly controlled parameters, such as for example temperature and energy density, to reduce the uncertainty regarding the origin of nucleation. In this paper, we report a new experimental setup designed to study NPLIN. After a full technical description of our own setup, we will illustrate the different functionalities of our device through results on glycine. Glycine crystals obtained through NPLIN, nucleate at the meniscus and exhibit different morphologies. Nucleation efficiency as a function of the supersaturation of the solution used and the LASER beam energy density have also been established on a large number of samples with all other parameters held constant.

## 1. Introduction

There is tremendous pressure on the pharmaceutical industry to understand the polymorphism of drugs in order to control and produce the most stable and effective polymorphs. The complete knowledge of the molecule polymorph stability is required for getting Food and Drugs Administration (FDA) approval in case of solid state formulation. However, despite the FDA approval, unstable polymorphs have inadvertently been placed on the market (Datta, 2004). There is a growing awareness of the consequences of polymorphism or pseudo-polymorphism on the properties of drugs, such as their physical and chemical stability, solubility, dissolution rate, bioavailability, mechanical properties, and the resulting consequences on the manufacturing process (Rodriguez - Spons, 2004), (Huang 2004). Finally, the development of new generic drugs has induced new studies showing that polymorphism can play a significant role in the differentiation between the generic and the innovative form (Shekunov, 2000), (Mangin, 2009).

Ideally, the experimental study of polymorphism implies the control over polymorphic crystallization and mastery of the search for new polymorphs. Several methods have been developed for inducing crystallization using an external constrain on the system, including electric fields (Taleb, 2001), ultrasound, or light irradiation (Sun, 2006). In some cases, these methods enable spatial control or

temporal control the nucleation with varying success. Among these methods, the LASER-Induced Nucleation (LIN) has great potential. In the last years, LASER-induced nucleation experiments have been done on molecules, organic molecules, and salts. Table 1 summarizes, schematically, the different characteristics of the experimental setups currently available in the world.

The experimental setups considered in this paper are those for which a LASER has induced a nucleation of crystals after irradiation of a supersaturated solution or a liquid. Garetz *et al.* (Garetz, 1996) have called this phenomenon Non-Photochemical Laser-Induced Nucleation (NPLIN), while other authors use a variety of acronyms (see figure S1). We decided to extent the use of the acronym NPLIN for all the experiments, which respects the following equation (see figure S2). In that framework, we eliminate the crystalline growth experiments *via* a LASER beam for which the initial compound is already a crystalline material [see for example [Yoshikawa 2006b], [Sugiyama 2009]]. In this paper, the NPLIN acronym does not give any information on the nucleation mechanism and does not give any restriction on that mechanism, it just implies that there is no chemical transformation of the compound.

Four main sections can be used to describe the experimental setup: i) the LASER; ii) the sample holder; iii) the observation equipment; iv) the characterization technique. A small number of experiments have been performed using a Continuous Waves (CW) LASER, while the others were performed with a Pulsed LASER (P). Therefore we distinguish five experimental categories of the LASER setup: i) Pulsed, nanosecond focused LASER (P – ns – foc); ii) Pulsed, nanosecond non-focused LASER (P – ns – nfoc); iii) Pulsed, femtosecond focused LASER (P – fs – foc); iv) Pulsed, femtosecond non-focused LASER (P – fs – nfoc); v) Continuous wave, focused LASER (CW – foc).

The following wavelengths were used: 532, 780, 800, and 1064 nm. Figure 1 represents schematically the different sample holders, which differ in geometry (a bubble, an HPLC glass vials, a spectroscopic tube or an essay tube), affecting the focus of the beam through various ways (a camera, a lens, or the cylindrical wall of the essay tube), and in volume (from 2  $\mu$ l to 10 ml). Some of these sample holders are part of a multi-batch system. For some of them temperature is controlled (Table 1). The crystal analysis techniques have been classified in two main categories: i) the *in situ* ones, i.e. techniques which are embedded in the experimental set-up; ii) the *ex situ* ones, i.e. techniques which need to take away the crystalline material for performing the observation. In the characterization techniques, we have reported the methods used for identification of the crystal and / or polymorphic forms.

Furthermore, nucleation of glycine using NPLIN method, exhibits an interesting property, which is the capability to produce a particular polymorph according to the incident polarization of the LASER beam ((Sun, 2006), (Sun, 2008)). This was noticed only for glycine in a special range of supersaturation (1.45 – 1.65 at room temperature (RT)). In the range 1.45 – 1.65 at RT, the  $\alpha$  polymorph was produced using circular polarization (CP) and the  $\gamma$  polymorph was produced using linear polarization (LP) (Sun, 2006). A similar behavior has been noticed in the case of L - (+) - histidine (Sun, 2008).

Working in the context of the pharmaceutical polymorphism, we report in this paper a new experimental setup for a high throughput NPLIN under controlled experimental conditions. The first experimental device based on the Matic *et al* (Matic, 2004) experimental setup has quickly reached its limits in the context of a real control of the nucleation and crystallization using the NPLIN method. We have therefore established the needs for an NPLIN experiment in order to assure quality and reproducible measurements. After a brief description of the methodology necessary to perform a conclusive NPLIN method, and for illustrating the use of this new device, some results on glycine crystallization are presented and discussed. Using this device, we have properly demonstrated an effect of the LASER on glycine solutions and recorded the fast nucleation after exposure.

**Table 1** Description of the 15 NPLIN experimental setups.

Setup number	LASE R type <sup>[1]</sup>	Wave length (nm)	Sample holder number environment <sup>[2]</sup>	<i>In situ</i> observation technique <sup>[3]</sup>	<i>Ex situ</i> observation technique	Characterization technique <sup>[4]</sup>	Compounds	References <sup>[5]</sup>
M0	P - ns - nfoc	53, 2, 10, 64	8	SHG (5)		SHG (5), PXRD (2,3,5,6)	Glycine, Urea, Histidine, Glacial acetic acid	1,2,3,4, 5,6,7,8
M1	P - fs - foc	78, 80, 0	2 - m	CCD Camera (10,11,13)	Photography	Single – Crystal XRD (12) Fluorescence (11)	Lysozyme, Ribonuclease B, Sheep liver sorbitol dehydrogenase, Glucose dehydrogenase, Fructose dehydrogenase, Myoglobin, Paracetamol	9,10,11, 12,13
M2	P - fs - foc	80, 0	9 - c - m			Single – Crystal XRD	4-(dimethylamino)-N-methyl-4-stilbazolium tosylate	14,15
M3	P - fs - foc	80, 0	4	CCD Camera	Photography		Anthracene	16
M4	P - ns – nfoc P - ps - nfoc	53, 2, 10, 64	3 - m		Photography		Lysozyme, Bovine Pancreas Trypsin	17
M5	P - fs - foc	78, 0	2	CCD camera	Photography	Fluorescence (19)	Lysozyme, Thaumatine	18
M6	P - ps - nfoc	53, 2	6		Photography, Cross polarizer-analyzer		4'-n-pentyl-4-cyanobiphenyl	19

M7	P - ns - nfoc	53 2, 10 64	7		Photog raphy (23, 24)		KCl, KBr	20,21,2 2,23,24
M8	CW - foc	10 64	5	CCD camera	Photog raphy (26)	FTIR	Glycine	25,26,2 7
M9	CW - foc	10 64	2 - c	CCD Camera	Photog raphy	Morphol ogy	Glycine	28
M10	P - fs - foc	78 0	1	CCD Camera	Photog raphy	Morphol ogy	Glucose Isomerase	29
M11	P - ns - foc	53 2	2	CCD Camera	Photog raphy	Morphol ogy	KMnO <sub>4</sub> , (NH <sub>4</sub> ) <sub>2</sub> SO <sub>4</sub>	3031
M12	CW - foc	10 64	2	CCD Camera, Raman (34)	Photog raphy (33,34) Spectr oscopy (34)	Morphol ogy (33,34) Fluoresc ence (33,34) Raman (35)	Glycine, Lysoyme	32,33,3 4
M13	P - ns - foc	53 2	7	Light scattering turbidity analysis	AFM image		KNO <sub>3</sub>	35
M14	P - fs - foc	80 0	5	CCD Camera	Photog raphy	Morphol ogy, Single- Crystal XRD	Glycine	36
this work	P - ns - nfoc	53 2	10 - c - m	CCD Camera	Photog raphy	Morphol ogy, PXRD, Single - Crystal XRD	Glycine, Carbamazepine	this work, 37, 38

<sup>[1]</sup> LASER type: P = Pulsed, CW = Continuous Waves, ns = nano-second, fs = femto-second, ps = pico-second, nfoc = non focused, foc = focused.

<sup>[2]</sup> Sample holder environment: the numbers refers to figure 1, m = multi-batch, c = temperature control.

<sup>[3]</sup> *In situ* observation technique: SHG = Second Harmonic Generation.

<sup>[4]</sup> Characterization techniques of the molecule and/or the polymorphs crystallized: PXRD = Powder X-ray Diffraction, SCXRD = Single Crystal X-ray Diffraction, FTIR = Fast Transform Infrared Spectroscopy.

<sup>[5]</sup> 1 = (Garetz, 1996), 2 = (Zaccaro, 2001), 3 = (Garetz, 2002), 4 = (Matić, 2005), 5 = (Sun, 2006), 6 = (Sun, 2008), 7 = (Alexander, 2009a), 8 = (Knott, 2011), 9 = (Adachi, 2003), 10 = (Nakamura, 2007a), 11 = (Murai, 2010), 12 = (Yennawar, 2010), 13 = (Nakayama 2013), 14 = (Hosokawa, 2005), 15 = (Tsunesada, 2002), 16 = (Nakamura, 2007), 17 = (Lee, 2008), 18 = (Yoshikawa, 2009), 19 = (Sun, 2009), 20 = (Alexander, 2009), 21 = (Ward, 2009), 22 = (Ward, 2011), 23 = (Ward, 2012a), 24 = (Ward, 2012b), 25 = (Rungsimanon, 2010a), 26 = (Yuyama, 2012), 27 = (Nakayama 2013), 28 = [Yuyama, 2010], 29 = (Iefuji, 2011), 30 = (Soare, 2011), 31 = (Murai, 2011), 32 = (Yuyama, 2012), 33 = (Uwada, 2012), 34 = (Tsuboi, 2007), 35 = (Belloni, 2012), 36 = (Liu, 2013), 37 = (Spasojevic-de Biré, 2013), 38 = (Ikni, 2014).

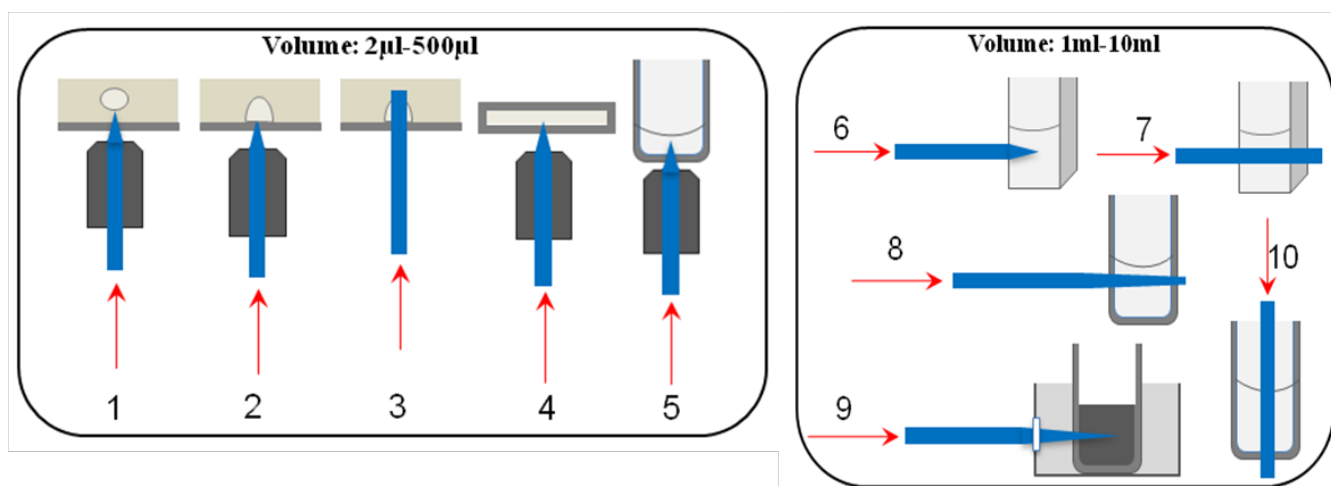


**Figure 1** Schematic representation of the different sample holders available in the NPLIN experimental setups. Sample holders 1 to 5 correspond to a volume of 2 to 500  $\mu\text{l}$ , while sample holders 6 to 10 correspond to a volume of 1 to 10 ml. Focusing is done through objectives (1, 2, 4, 5) or lens (6, 9). An unwanted focusing by a factor 1.53 is due to a cylindrical essay tube in 8 (Matić, 2004). The LASER beam, whatever the wavelength is, is represented in blue color. A red arrow indicates the direction of the beam.

## 2. Material and methods

### 2.1. Experimental needs and solutions retained

Nucleation is a process whose outcome depends on a large number of factors, including ones that sometimes escape direct control. In particular, standard macroscopic thermodynamics and standard macroscopic kinetics do not apply, mainly because the nucleating medium is heterogeneous. Minor impurities also certainly have a role. Therefore, it is crucial to be able to perform numerous experiments under the same experimental conditions. Considering the influencing factors in the nucleation process, primarily temperature should be controlled and monitored, and the energy density of the LASER beam also has to be monitored. Furthermore, a visual monitoring of crystallization through microphotographs is necessary. Taking into account these general needs, a multipurpose high-throughput experimental setup is to be designed and built with a special care being done on the software (see figure S3). We chose to use different methods for characterization: *in situ* by a visual control of the morphology, *ex situ* after filtering of the solution, through Powder X-Ray Diffraction (PXRD) and Single Crystal X-ray Diffraction (SCXRD) measurements and Scanning Electron Microscopy (SEM) observations. Figures 2 and 3 show schematic representations of our new experimental device while figure 4 shows how the experimental design was implemented.

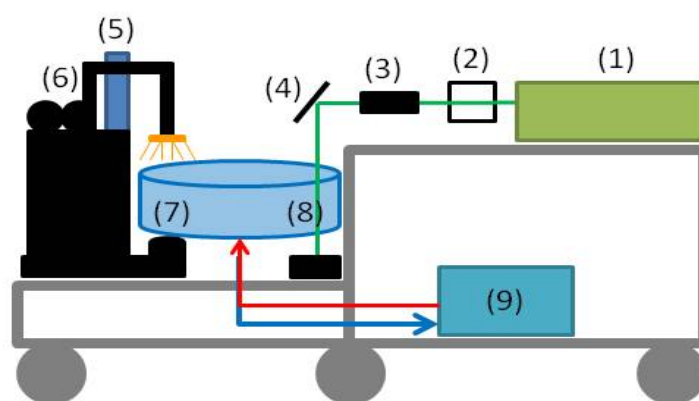


**Figure 2** Schematic representation of the experimental setup. (1) LASER (2) Wattmeter (3) Condensor (4) Mirror (5) Camera, (6) Inverted microscope (7) Observation area (8) Exposition area (9) Cryothermostat. Red arrow: in flow, blue arrow: out flow. The whole setup is mounted on a trolley (grey).

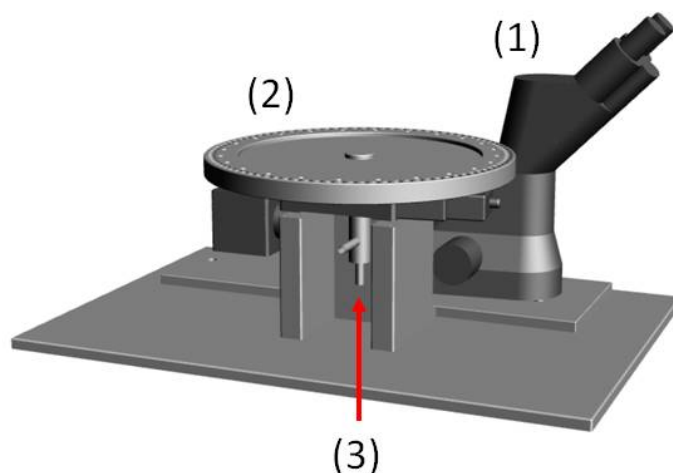


**Figure 3** 3D Computed Aided Design of the carousel. (1) Inverted microscope (2) 90 holes for HPLC tubes (3) Heat transfer fluid circulation.

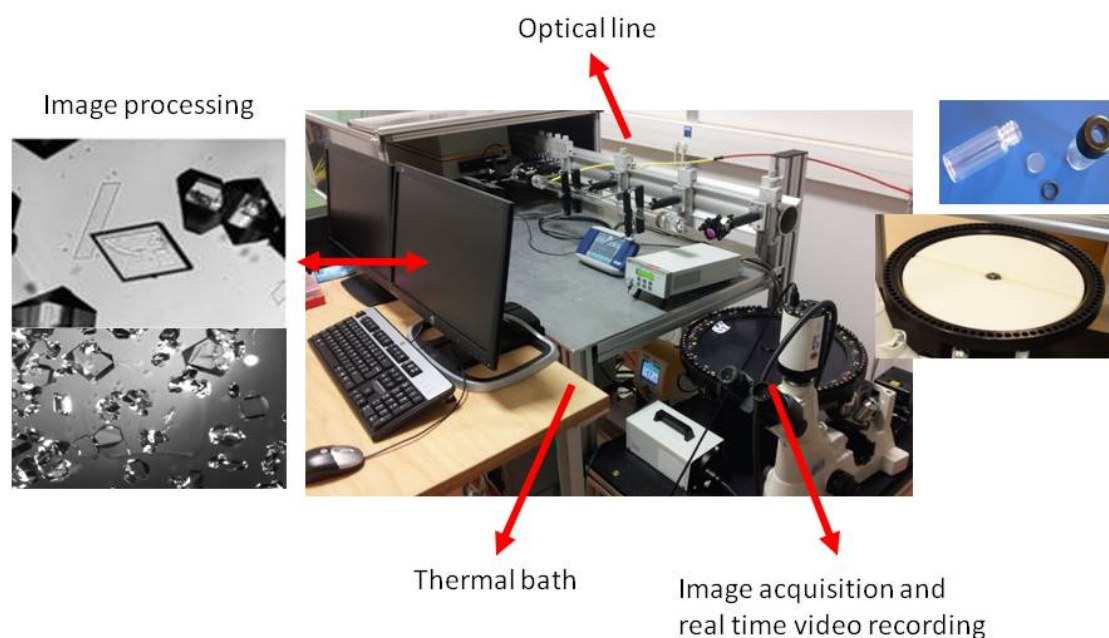


**Figure 4** Photographs of the experimental setup

Following is a detailed description of the experimental setup. A rotative sample holder, called carousel, for 90 HPLC glass vials with a radius of 340 mm under control of a step by step motor from Newport Micro Control® (URS100BCC) is designed and built. The carousel is an assembly of three pieces, which allow water flow in order to control the temperature of the exposed and monitored samples. Because of the rotative configuration, the input and output water flows are on the same axis in two different pipes. Inside the carousel, an intermediate piece was created with two levels in order to manage input and output flows (see figure S5). The water flow is controlled by a cryothermostated bath from Lauda® in a closed circuit. The actual temperature control device operates in a range from 278 to 333 K. Three temperature sensors permit temperature monitoring; one measures the temperature at the entrance of the pipe, another at the output of the pipe, and the third one is mobile and can be inserted inside the carousel. The change of the fluid type could allow the use of the system at lower or higher temperatures. We have installed a LASER Nd:YAG using a wavelength of 532 nm,



(beam 7 mm in diameter, pulse of 7 ns, 300 mJ). The LASER beam at 532 nm is reduced through a beam reducer in order to increase the LASER energy density. The reduction of the LASER beam diameter could be done in two ways: i) a laboratory made telescope with a Nitrogen gas circulation for avoiding plasma discharge at the focal point reduces the beam diameter by a factor 2; ii) a commercial condenser HEBX-3X from Melles Griot<sup>®</sup> reduces the beam by a factor 3. The beam is directed on the solution using one mirror at the end of the optic line. This vertical configuration was chosen because the insertion of the beam through cylindrical face induces strong focalization by a factor 2 (Figure 1, sample holder n° 8). This focalization is not controlled and has to be avoided. We have therefore decided to use chromatography tubes exposed from the top through a glass plate. For safety of experimenters the vertical beam is directed to the ground. This issue also allows us to minimize the compounds quantity in case of necessity. In order to know the exact LASER energy density received by the sample, a homemade glass plate is put just after the shutter to collect 3 % of the outgoing beam; a wattmeter from Excell Technology France<sup>®</sup> (QE25LB-S-MB) is used to continuously monitor at every time the beam power. To precisely control the exposure time, a programmable shutter Thor Lab<sup>®</sup> (SC05 / SH 10) is inserted inside the beam line. A Glan polariser with a Quarter Wave plate from Melles Griot<sup>®</sup> can be added to modify the polarization and produce elliptical or circular polarization. The *in situ* crystallization observation is performed using an inverted microscope, (Nikon<sup>®</sup> MA 100) using a CCD camera (Q-imaging) connected to the automated system. The microscope is placed at 180 ° of the LASER exposure path, enabling the analysis of the solution one second after exposure to the LASER beam. All the equipment is installed on a cart that includes space for the LASER and its supply circuit. A mobile hood can be installed during the experiments for the safety of the experimenters.

## 2.2. Automation

A computer program was developed to control and manage each step of the experiment, using LABVIEW framework (National Instruments<sup>®</sup>). Firstly, the user programs the control of peripheral instruments, such as bath temperature. Then the exposure sequence is programmed through an Excel (Microsoft<sup>®</sup>) file, which allows input of sample information, such as LASER exposure characteristics and the observation time. From this point, there are three modes: manual, automatic and semi-automatic. The manual mode is fully managed by the operator allowing, step by step, exposure and the possibility to record observation for a long time. The automatic mode executes the programmed sequence in the Excel file. The semi-automatic sequence works as the automatic one but the parameters related to the LASER exposure, observation setup and temperature can be changed by the experimenters just before running a sequence. This software allows a real time recording of temperature and beam intensity while exposure and observation steps are performed.

## 2.3. Glycine nucleation and crystallization

### 2.3.1. Sample preparation

Supersaturated glycine solutions were prepared by dissolution of glycine in distilled water. The solutions used to demonstrate the NPLIN effect were prepared in the range of supersaturation constant ( $C=S/S_0$ ) from 1.0 to 2.0 at a temperature of 290 K using the solubility curve published by Yang (Yang, 2008) (figure 5). The initial compound, tested before dissolution using PXRD, was  $\gamma$  polymorph except for figures 7, 8 and 10 where an initial  $\alpha$  glycine polymorph was used (See figure S4).

A mass of glycine corresponding to the supersaturation rate at 290 K calculated using glycine solubility curve was added in HPLC tubes, then 1 mL of water was added. The tube was stored inside the sample holder at a temperature of 333 K in order to dissolve glycine by thermal diffusion and concentration gradient convection. The dissolution route is the following: samples were kept for 36h at 291 K then a cooling slope of 0.2°C/min is applied until the temperature of exposure (291 K) was reached. That temperature was maintained for 12h before LASER exposure.

### 2.3.2. LASER-induced nucleation

The Nd: YAG LASER was used in a range of settings that supplies energy from 50 mJ to 320 mJ. The exposure time was one minute. The beam has a vertical linear polarization at 99%. A quarter wave plate was used to produce circularly polarized light. It was controlled using a Glan polarizer checking the Malus' law (see the biography from Chappert (Chappert, 1977)) before the exposure of the sample to the LASER.

### 2.3.3. Polymorph characterization

The determination of the initial powder polymorph or that obtained using the LASER was accomplished using PXRD. SEM experiments enable the characterization of the morphologically the initial powder. The crystals obtained after spontaneous nucleation or NPLIN were grinded in a mortar. PXRD data were recorded at room temperature on a Brüker<sup>®</sup> D2 Advance powder diffractometer. For morphological characterization, single crystals were probed using a Brüker<sup>®</sup> D8 single crystal diffractometer at room temperature.

## 3. Results and discussions

### 3.1. A methodology for NPLIN study

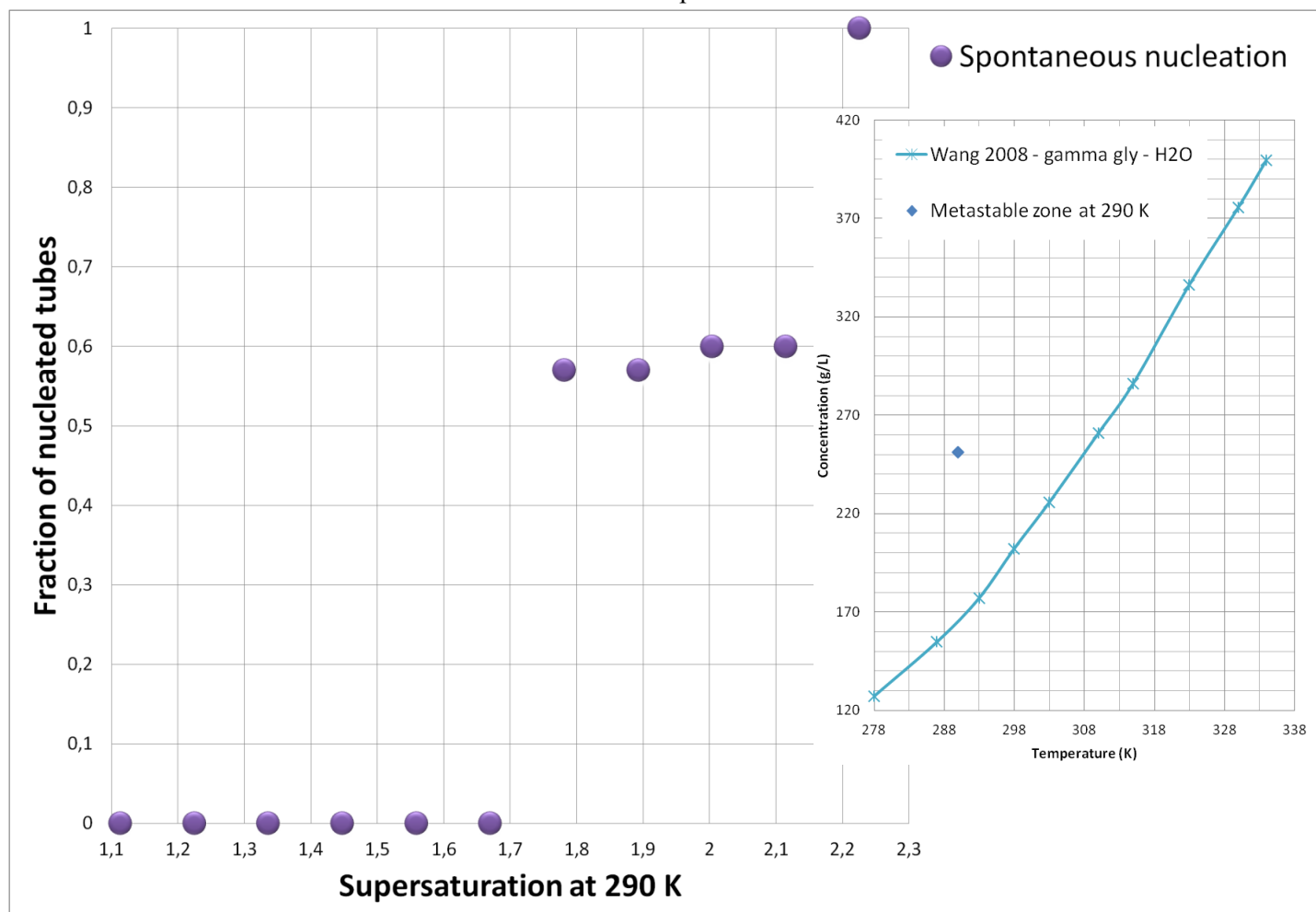
The key point of any NPLIN study is to demonstrate that the LASER has induced the nucleation while without the LASER there would be no nucleation. For achieving this task three steps have to be performed prior to the NPLIN experiments: i) Characterization of spontaneous crystallization under similar conditions (method of dissolution, temperature, supersaturation, pH, ...), as those used for the NPLIN method, leading to the determination of the induction time in spontaneous crystallization; ii) Determination of the solubility curve in similar conditions; iii) Determination of the metastable zone. The potential to achieve thermodynamically metastable states is a characteristic feature of first order phase transitions (Kaschchiev, 1991). Starting from the initial phase, supersaturating the solution during a time interval  $t_i$  leads to the formation of a new phase materialized by the appearance of crystals. The time interval  $t_i$  separating these two phases is referred to as the induction time and is used as a measure of the ability of the system to remain in a metastable equilibrium. It can therefore be used to determine the metastable limit of the initial phase. Indeed, it allows us to determine the critical supersaturation below which the initial phase can stay long enough without losing its metastability. These tasks have been extensively described by Revalor *et al* (Revalor, 2010). Therefore, knowing for a given molecule in a given solvent, the temperature, the supersaturation and the induction time, NPLIN experiments can be performed.

### 3.2. Application to glycine

Glycine has six polymorphs, three of them are known at room temperature from many years such as  $\alpha$  ((Albrecht, 1939), (Marsh, 1958)),  $\beta$  ((Ficher, 1905), (Iitaka, 1958))  $\gamma$  ((Iitaka, 1958), (Iitaka, 1960), (Iitaka, 1961)). Three other polymorphs ( $\delta$ ,  $\epsilon$ ,  $\zeta$ ) could be produced from high pressure experiments, starting from the  $\gamma$  form ((Boldyreva, 2003b), (Goryainov, 2006), (Dawson, 2011)). The most stable form at room temperature and ambient pressure is the  $\gamma$  form but the kinetically favored form at room temperature is  $\alpha$  (Boldyreva, 2003b). The polymorph  $\gamma$  is formed in acidic or basic solution (Yu, 2002) and in deuterated solutions (Iitaka, 1961). Using NPLIN, with a nano-second pulsed LASER the  $\gamma$  form was unexpected produced (Zaccaro, 2001) and selectively produced using polarization (Garetz, 2002), (Sun, 2006) or a femto-second pulsed LASER (Liu, 2013). Glycine has also been crystallized by NPLIN with a femto-second continuous wave LASER ((Rungsimanon, 2010), (Uwada, 2012), (Yuyama, 2012)).

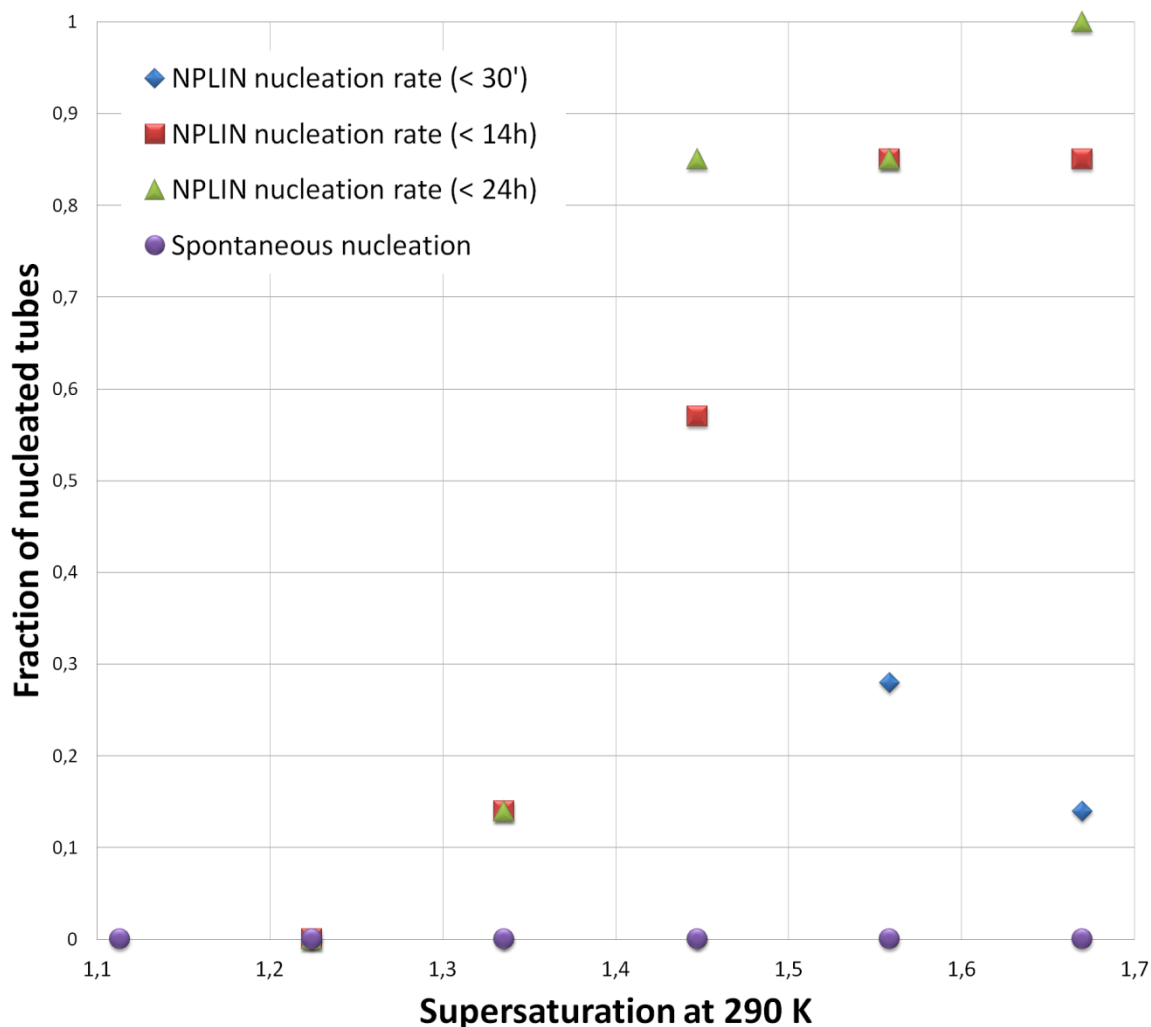
The metastable zone at 290 K is determined according to the methodology described below. This temperature was chosen to enable comparison with the NPLIN results of Sun *et al* (Sun, 2006), in which the polarization switching phenomenon was observed only at this temperature when using the

532 nm wavelength. Used as a reference, the solubility curve has been determined by Yang *et al* (Yang, 2008) (figure 5). The spontaneous nucleation for a range of supersaturations (figure 5) has been studied after 7 days. If  $n$  samples nucleate, the nucleation fraction is then given by  $n/N$ .  $N$  is reported on figure 5. Observations have been made after 36 hours and after 168 hours. From a thermodynamic point of view, for a supersaturation range between  $\beta=110\%$  and  $\beta=168\%$  and for a time less than 168 hours, one can consider that we are in the metastable zone. This limit is indicated by a blue point in figure 5-insert. Therefore, the critical supersaturation is  $\beta_{c, 290}(168) = 168\%$ . This illustrates how the limit of the metastable zone is dependent of the time of observation.



**Figure 5** Spontaneous nucleation efficiency of glycine at 290 K after 168 hours (one week). a) solubility curve of gamma glycine (Yang, 2008) and limit of the metastable zone (blue point). b) Spontaneous nucleation efficiency. Each point represents the results of 10 tubes.

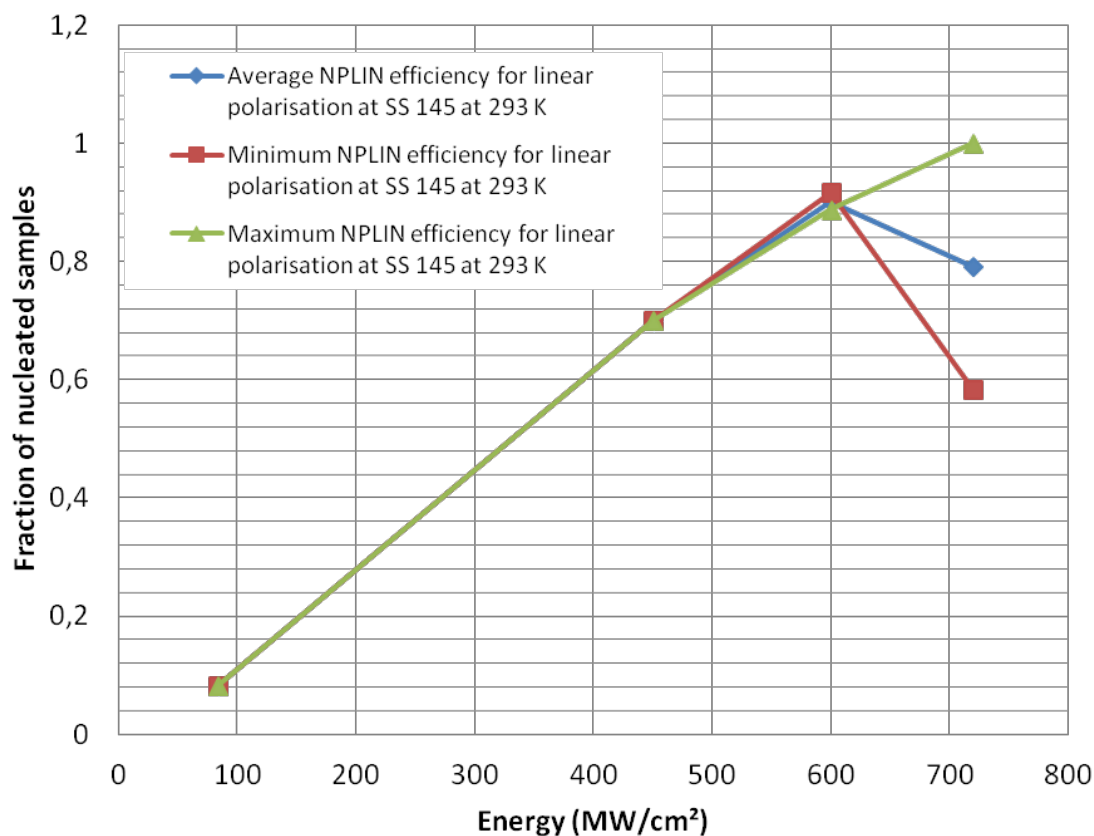
Using the semi-automatic mode, we have performed at a given supersaturation, LASER energy, and linear polarization number of experiment of nucleation induced by LASER. The results are reported in figure 6. The frequency of nucleated samples was recorded several times after exposure to the LASER (figure 6) through a microscopic observation checked by visual observation in the case of a nucleation starting at the meniscus in the geometry described in figure 1, sample holder n° 10.



**Figure 6** NPLIN Nucleation efficiency of aqueous glycine solutions at 290 K at different moment after irradiation. The  $t_0$  corresponds to the end of the LASER exposure (exposure time = 60s, energy = 680 MW/cm<sup>2</sup>, linear polarization). Each point represents the results of 10 samples.

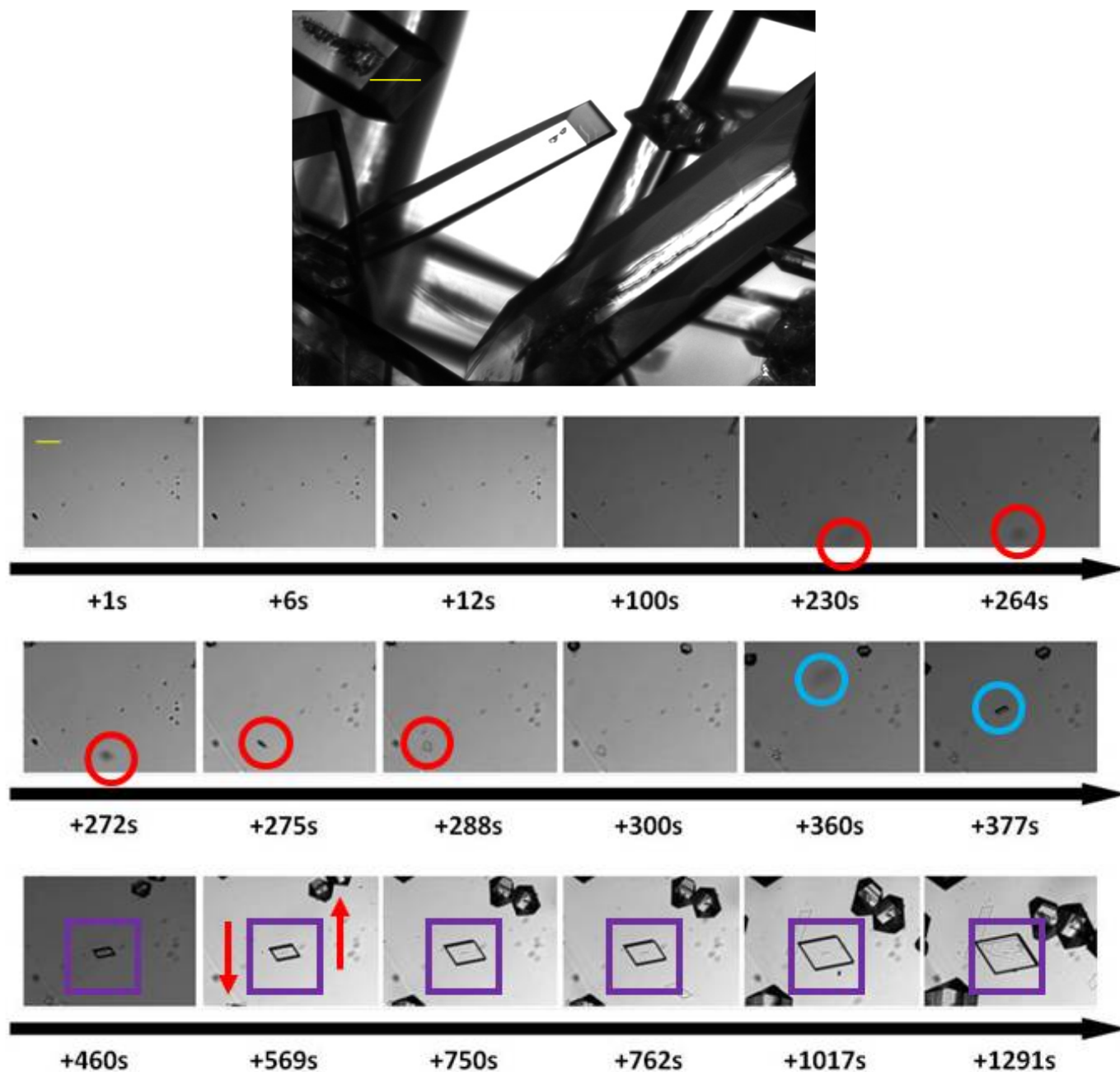
From this figure, it is clear that the LASER has induced the nucleation in the metastable zone. Below the supersaturation of 1.68, no spontaneous nucleation was recorded up to 168 h whereas using NPLIN, nucleation occurred quickly reducing the induction time (in hours) by at least a factor 7. Below supersaturation of 1.34 no NPLIN nucleation was recorded, confirming the results of the Garetz group [Sun, 2006] in this range, with a similar energy (460 MW/cm<sup>2</sup> for  $\lambda = 1064$  nm). The nucleation efficiency according to the injected power inside the solution (MW/cm<sup>2</sup>) was reported (figure 7). Up to an energy density of 600 MW/cm<sup>2</sup>, the average efficiency increased but dropped for energies up to 720 MW/cm<sup>2</sup>. This figure, based on two experiments done with the same parameters at two different moments shows a good reproducibility till 600 MW.cm<sup>-2</sup> and express a divergence at the highest energy.

Using the manual mode, we have observed optically the spontaneous (figure 8a) and the NPLIN crystallization (figure 8b). Our sample holder (figure 1, n° 9) is the only one for which the LASER beam goes through the air / solution interface (meniscus). One can observe (red circle) a shadow of a crystal, which falls down from the concave meniscus. The microscope objective was focused on the bottom of the HPLC glass vials. Later one can observe (blue circle) another crystal, which falls down to the bottom of the tube. The crystal growth can be observed for crystal (blue circle) from  $t_{\text{NPLIN}} = 360$  s to  $t_{\text{NPLIN}} = 1291$  s.



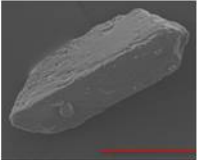
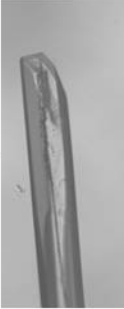
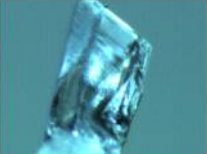
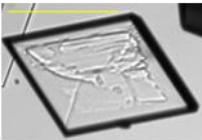
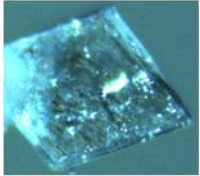
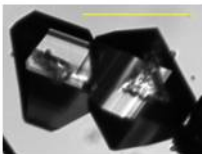
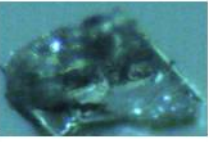
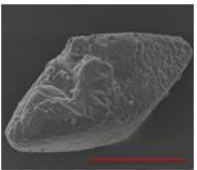


**Figure 7** NPLIN Nucleation efficiency of aqueous glycine solutions at various density of energy (83, 450, 600 and 720 MW/cm<sup>2</sup>) for a supersaturation of 1.45 for two different experiments. The average efficiency is plotted in blue. The number of samples used for each point is indicated in red.

A complete video is available in Supplementary Materials. Morphology of these crystals is completely different (figure 9). The photographs extracted from the film show that the complete crystallization is achieved in about 20 minutes. These recorded images are reproducible from one sample to another. The first observable crystals can be formed quickly after the exposure time. In a second period, crystals falling from the meniscus arrived after about 4 minutes when they reached a critical size subjected to gravity. The meniscus, as a nucleation site in HPLC glass vials, has been reported by Liu *et al.* (Liu, 2013). They used a femtosecond LASER focused at different places (meniscus, bottom of the HPLC glass vials and in the volume of the solution) and showed that meniscus is a highly preferential place for nucleation.



**Figure 8** User manual mode to follow the crystallization. a) Spontaneous crystallization  $\beta_{290} = 200\%$ . Crystallization was observed using a 2.5x Nikon objective. b) NPLIN and crystallization. The  $t_0$  corresponds to the end of the LASER exposure (exposure time = 60s, energy = 1,4 GW/cm<sup>2</sup>, linear polarization, supersaturation = 1.6 at 290K). Crystallization was observed using a 5x Nikon objective. The red and blue circles show the fall of a crystal coming from the meniscus shown by the shadow. The violet square shows the growth of a crystal; the same behavior is observed for two different morphologies shown by red arrows. The scale is given by the yellow line and represents 104  $\mu\text{m}$ .



Initial polymorph		Spontaneous crystallization		NPLIN crystallization		
$\alpha$						$\alpha$
						$\alpha$
$\gamma$						$\alpha$

**Figure 9** Polymorphic identification of morphologies of glycine. Initial polymorph powder (SEM photography); spontaneous and NPLIN crystallization: 1<sup>st</sup> column microphotography from our experimental device, 2<sup>nd</sup> column single crystal diffractometer photography. Crystals are identified through single crystal diffraction. The scale is given by the colored line (yellow represents 104  $\mu\text{m}$ , red 200  $\mu\text{m}$  and blue 52  $\mu\text{m}$ ).

The polymorphs have been identified through single crystal X-ray diffraction. The spontaneous nucleation gives always the same rod-like morphology as described previously in the literature (Toth, 2005), (Srinivasan, 2007), (Rabesiaka, 2010), (Srinivasan, 2011). The three distinct morphologies obtained by NPLIN are  $\alpha$  glycine polymorph (figure 9). Comparison between spontaneous morphologies (figure 8a) and NPLIN morphologies (figure 8b, 9) shows the formation of morphologies not observed in  $\alpha$  spontaneous nucleation. The LASER has therefore an impact on the morphology. The morphology reported in the second line looks similar to those obtained by Masuhara *et al.* (Masuhara, 2011) with a CW LASER at 1064 nm. The two other morphologies have not been clearly reported through an NPLIN experiment. Despite the fact that the single crystal experiment have clearly identified an  $\alpha$  polymorph, one cannot exclude that some  $\beta$  crystals exists, since the NPLIN morphology reported in the third line of table 5 is quite similar to those reported by Ferrari *et al.* (Ferrari, 2003) growth from a mixture of water and ethanol. A transformation from  $\beta$  to  $\alpha$  is not excluded since polymorphic transformation has been reported in solution (Srinivasan, 2008) keeping the same morphology.

We have shown that the LASER has an effect on the outcoming morphologies. The influence of the supersaturation linked with the polarization is also studied (figure 10). Our results show an influence of the circular polarization above the supersaturation of 1.56 with increasing the  $\gamma$  nucleation. Below this value, there is a high nucleation rate of the  $\alpha$  polymorph. This behavior is observed for the linear polarization whatever the supersaturation is. The influence of the polarization is not as strong as reported by Sun *et al.* (Sun, 2006). This could be due to the incoming beam direction, which was modified in our new device (See figure 1 n°8 (Garetz group), n°10 (this work)) implying an higher energy for Sun *et al.* (Sun, 2006).

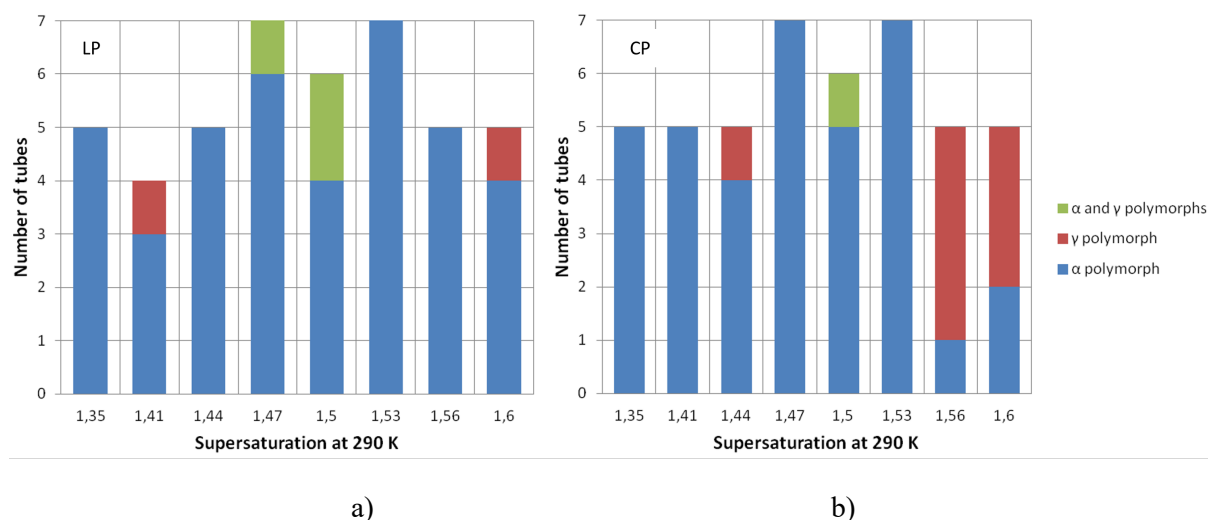


**Figure 10** Nucleation rate of the  $\alpha$  and the  $\gamma$  polymorphs according to the supersaturation ratio at 290 K at an energy of  $910 \text{ MW}\cdot\text{cm}^{-2}$  a) linear polarization (LP) b) circular polarization (CP).

#### 4. Conclusions

In this paper, we have adopted a new definition of the experiments which belong to a Non - Photochemical Light-Induced Nucleation (NPLIN) despite the fact that some authors have not use this terminology in their papers. We consider that a LASER, which induces nucleation of the compound in solution or in a liquid state, belongs to an NPLIN experiment if the molecules forming the crystal obtained are not chemically modified by a light matter interaction. A zwitter ionic form is considered chemically similar in our definition. We have reviewed the different experimental setups available in the world leading to 15 setups, 9 sample holders types – that is to say 40 references including 3 reviews papers ((Masuhara, 2011a), (Sugiyama, 2009), (Yoshikawa, 2014)). Based on this literature and on our own Laboratory experience, we have designed a new experimental setup. This setup permits to study a large number of samples (90) in highly controlled conditions (temperature, LASER energy density, time exposure, air, moisture). A methodology has been developed based on the systematic study of the metastable zone prior to LASER exposure. Using the knowledge of this metastable zone, we have performed NPLIN of samples. We have chosen to illustrate the capacity of our experimental setup on glycine, the most studied compound *via* NPLIN technique. Results show that LASER stimulates the nucleation inside the metastable zone (critical supersaturation constant  $\beta_{c,290} (168) = 168\%$ ) where no spontaneous nucleation occurs. Real time recording video shows a short induction time (some minutes in order to have a crystal detection with the camera mounted on a microscope). Particular morphologies of crystals induced by the LASER have been observed, which are not produced by spontaneous nucleation. All the crystals formed have been identified as belonging to the  $\alpha$  polymorph through single crystal X-ray diffraction experiments. Furthermore, we have observed that glycine nucleates at the air / solution interface before falling down to the bottom of the tube. Nucleation efficiency *via* a LASER in a non-photochemical way has been evidenced at different supersaturations or laser beam energy. The higher is the supersaturation constant value the better the nucleation efficiency is. A maximum efficiency is observed for the glycine nucleation as a function of the LASER energy density despite a slight reproducibility divergence for highest energy. Formation of  $\gamma$  glycine polymorph with circular polarization, at high supersaturation is favored. Using the new experimental device reported in this paper, we are currently working on carbamazepine (Ikni, 2014) and sulfathiazole (Spasojevic-de Biré, 2014), two drugs, which are highly polymorphic.

**Acknowledgements** We would warmly thank Stephane Veessler (CINaM, UMR 7325 CNRS Campus de Luminy, Marseille, France) for fruitful discussion. We thank the technical support of the EM2C Laboratory (Erica Jean-Bart and Jérôme Beaunier) for their very efficient participation in the project. We also thanks Jelena Matić (former PhD at Polytechnic University of New York, USA) and



Nour Eddine Ghermani (UMR 8612, U-PSud, Châtenay-Malabry, France) for their useful suggestions on the manuscript. This project is supported by an ANR P2N grant 2010, “NPLIN\_4\_drug”.

**Supplementary Material.** Table S1: Acronyms used in various papers for describing the LASER induced nucleation experiments. Table S2: Needs and solution developed in our high-throughput NPLIN experimental setup. Table S3: Initial polymorph used in this paper and experimental conditions. Figure S1: Non-Photochemical LASER-induced Nucleation experiments definition. Figure S2: Schematic representation of the fluid inside the carousel setup. Figure S3: A movie of the crystal nucleation just after LASER exposure.

## References

- [Adachi, 2003] Adachi, H., Takano, K., Hosokawa, Y., Inoue, T., Mori, Y., Matsumura, H., Yoshimura, M., Tsunaka, Y., Morikawa, M., Kanaya, S., Masuhara, H., Kai, Y. & Sasaki, T. (2003). *Jpn. J. Appl. Phys.* **42** L798 - L800.
- [Albrecht, 1939] Albrecht, G. & Corey, R. B. (1939). *J. Am. Chem. Soc.*, **61**, 1087 - 1103.
- [Alexander, 2009] Alexander, A. J. & Camp P. J. (2009). *Cryst. Growth Des.*, **9**, 958 - 963.
- [Boldyreva, 2003] Boldyreva, E. V., Drebuschak, T. N. & Shutova, E. S. (2003). *Z. Kristallogr.* **218**, 366-376.
- [Chappert, 1977] Chappert A. (1977) Paris, Vrin
- [Datta, 2004] Datta, S. & Grant, D., J., W. (2004). *Nat. Rev. Drug Discovery* **3**, 42 - 57.
- [Dawson, 2005] Dawson, A., Allan, D., R., Belmonte, S., A., Clark, J., David, W., I., F., McGregor, P., A., Parsons, S., Pulham, C., R. & Sawyer, L. (2005). *Cryst. Growth Des.*, **5**, 1415 - 1427.
- [Duffus, 2009] Duffus, C., Camp, P., J. & Alexander, A., J. (2009). *J. Am. Chem. Soc.* **131**, 11676 - 11677.
- [Fischer, 1905] Fischer, E. (1905). *Ber. dtsh, chem. Ges.* **38**, 2917.
- [Ferrari 2003] Ferrari, E., S., Davey, R., J., Cross, W., I., Gillon, A., L. & Towler, C., S. (2003) *Cryst. Growth Des.*, **3**, 53 - 60
- [Garetz, 1996] Garetz, B., A., Aber, J., E., Goddard, N., L., Young, R., G. & Myerson, A. S. (1996). *Phys. Rev. Lett.*, **77**, 3475 - 3476
- [Garetz 2002] Garetz, B. A. & Matić, J.,(2002). *Phys. Rev. Lett.*, **89**, 175501.
- [Goryainov, 2006] Goryainov, S.,V., Boldyreva, E.,V. & Kolesnik, E., N. (2006). *Chem. Phys. Lett.* **419**, 496 – 500.
- [Hosokawa, 2005] Hosokawa, Y., Adachi, H., Yoshimura, M., Mori, Y., Sasaki, T. & Masuhara, H. (2005). *Cryst. Growth Des.*, **5**, 861 - 863.
- [Huang, 2004] Huang, L., F. & Tong, W., Q. (2004). *Adv Drug Deliver Rev*, **56**. 321 - 334
- [Iefuji, 2011] Iefuji, N., Murai, R., Maruyama, M., Takahashi, Y., Sugiyama, S., Adachi, H., Matsumura, H., Murakami, S., Inoue, T., Mori, Y., Koga, Y., Takano, K. & Kanaya, S. (2011). *J. Cryst. Growth*, **318**, 741 - 744.
- [Iitaka, 1958] Iitaka, Y. (1958). *Acta Cryst.*, **11**, 225 - 226.
- [Iitaka, 1960] Iitaka, Y. (1960). *Acta Cryst.*, **13**, 35 - 45.
- [Iitaka, 1961] Iitaka, Y. (1961). *Acta Cryst.*, **14**, 1 - 10.
- [Ikni, 2013] Ikni, A., Clair, B., Scoufflaire, P., Veesler, S., Gillet, J-M., El Hassan, N. Dumas, F. & Spasojević-de Biré, A. (2014). submitted to *Cryst. Growth Des.*
- [Izmailov, 1999] Izmailov, A., F., Myerson, A., S. & Arnold, S. (1999). *J. Cryst. Growth*, **196**, 234 - 242.
- [Jacob, 2012] Jacob, J., A., Sorgues, S., Dazzi, A., Mostafavi, M. & Belloni, J. (2012). *Cryst. Growth Des.*, **12**, 5980 – 5985.
- [Knott, 2011] Knott, B., C., LaRue, J., L., Wodtke, A., M., Doherty, M., F. & Peters, B. (2011). *J. Chem. Phys.*, **134**, 171102.
- [Lee, 2008] Lee, I., S., Evans J., M., B., Erdemir, D., Lee, A., Y., Garetz, B., A., & Myerson, A., S. (2008). *Cryst. Growth Des.* **8**, 4255 - 4261
- [Liu, 2013] Liu, T., H., Uwada, T., Sugiyama, T., Usman, A., Hosokawa, Y., Masuhara, H., Chiang, T., W., & Chen, C., J. (2013). *J. Cryst. Growth*, **366**, 101 - 106.

- [Matić, 2004] Matić, J. PhD (2004). Polytechnic University of New York
- [Matić, 2005] Matić, J., Sun, X. & Garetz, B., A. (2005). *Cryst. Growth Des.*, **5**, 1565 - 1567.
- [Mangin, 2009] Mangin, D., Puel, F. & Veessler, S. (2009). *Org. Process Res. Dev.* **13**, 1241 - 1253
- [Marsh, 1958] Marsh, R. E., (1958). *Acta Cryst.*, **11**, 654-663.
- [Masuhara, 2011] Masuhara, H., Sugiyama, T., Rungsimanon, T., Yuyama, K., Miura, A. & Tu, J., R. (2011). *Pure Appl. Chem.*, **83**, 869 – 883.
- [Murai, 2010] Murai, R., Yoshikawa, H., Y., Takahashi, Y., Maruyama, M., Sugiyama, S., Sasaki, G., Adachi, H., Takano, K., Matsumura, H., Murakami, S., Inoue, T. & Mori, Y. (2010). *Appl. Phys. Lett.*, **96**, 043702.
- [Murai, 2011] Murai, R., Yoshikawa, H., Y., Hasenka, H., Takahashi, Y., Maruyama, M., Sugiyama, S., Adachi, H., Takano, K., Matsumura, H., Murakami, S., Inoue, T. & Mori, Y. (2011). *Chem. Phys. Lett.*, **510**, 139 - 142.
- [Nakamura, 2007a] Nakamura, K., Sora, Y., Yoshikawa, H., Y., Hosokawa, Y., Murai, R., Adachi, H., Mori, Y., Sasaki, T. & Masuhara, H. (2007). *Appl. Surf. Sci.*, **253**, 6425 - 6429.
- [Nakamura, 2007b] Nakamura, K., Hosokawa, Y. & Masuhara, H. (2007). *Cryst. Growth Des.*, **7**, 885 - 889.
- [Nakayama, 2013] Nakayama, S., Yoshikawa, H., Y., Murai, R., Kurata, M., Maruyama, M., Sugiyama, S., Aoki, Y., Takahashi, Y., Yoshimura, M., Nakabayashi, S., Adachi, H., Matsumura, H., Inoue, T., Takano, K., Murakami, S., & Mori, Y. (2013). *Cryst. Growth Des.* **13**, 1491 – 1496.
- [Rabesiaka 2010] Rabesiaka, M., Sghaier, M., Fraise, B., Porte, C., Havet, J.-L. & Dichi, E. (2010). *J. Cryst. Growth*, **312**, 1860 – 1865.
- [Revalor 2010] Revalor, E., Hammadi, Z., Astier, J-P, Grossier, R., Garcia, E., Hoff, C., Furuta, K., Okustu, T., Morin, R., & Veessler, S. (2010). *J. Cryst. Growth*, **312**, 939 – 946.
- [Rodriguez-Spons, 2004] Rodriguez-Spong B., Price C., Jayasankar A., Matzger A.,J. & Rodriguez-hornedo N. (2004). *Adv Drug Deliver Rev*, **56**, 241-274
- [Ruugsimanon, 2010] Rungsimanon, T., Yuyama, K., Sugiyama, T., Masuhara, H., Tohnai, N. & Miyata, M. (2010). *J. Phys. Chem. Lett.*, **1**, 599-603.
- [Shekunov, 2000] Shekunov, B.,Y. & York, P., (2000). *J. Cryst. Growth*, **211**, 122 – 136.
- [Soare, 2011] Soare, A., Dijkink, R., Pascual, M., R., Sun, C., Cains, P., W., Lohse, D., Stankiewicz, A., I. & Kramer, H., J., M., (2011). *Cryst. Growth Des.*, **11**, 2311 - 2316.
- [Spasojević - de Biré, 2013] Spasojević - de Biré, A. (2013). *International Innovation*, 45 – 49.
- [Spasojević - de Biré, 2014] Spasojević - de Biré A. Li, W., Ikni, A. (2014). unpublished results.
- [Srinivasan 2007] Srinivasan, K. & Arumugam, J. (2007). *Opt. Mater.* **30**, 40–43.
- [Srinivasan 2008] Srinivasan, K. (2008). *J. Cryst. Growth*, **311**, 156 - 162.
- [Sugiyama, 2009] Sugiyama, T., Adachi, T. & Masuhara, H. (2009). *Chem. Lett.* **38**, 482-483
- [Sun, 2006] Sun, X. & Garetz, B., A. (2006). *Cryst. Growth Des.*, **6**, 684 - 689.
- [Sun, 2008] Sun, X., Garetz, B., A. & Myerson, A., S. (2008). *Cryst. Growth Des.*, **8**, 1720 – 1722.
- [Sun, 2009] Sun, X. & Garetz, B., A. (2009). *Phys.Rev. E*, **79**, 021701.
- [Taleb, 2001] Taleb, M., Didierjean, C., Jelsch, C., Mangeot, J.P. & Aubry, A. (2001). *J. Cryst. Growth*, **232**, 250 - 255.
- [Toth 2005] Toth, J., Kardos-Fodor, A. & Halasz-Peterfi, S., (2005) *Chem. Eng. Process.*, **44**, 193 – 200.
- [Tsuboi 2007] Tsuboi, Y., Shoji, T. & Kitamura, N. (2007). *Jpn. J. Appl. Phys.* **46**, L1234 - L1236.
- [Uwada 2012] Uwada, T., Fuji, S., Sugiyama, T., Usman, A., Miura, A., Masuhara, H., Kanaizuka, K. & Haga, M. (2012). *Appl Mater Interfaces*, **4**, 1158-1163.
- [Ward 2009] Ward, M., R., Ballingall, I., Costen, M., L., McKendrick, K., G. & Alexander, A., J. (2009). *Chem. Phys. Lett.*, **481**, 25 - 28.
- [Ward, 2011] Ward, M., R. Copeland, G., W. & Alexander, A., J. (2011). *J. Chem. Phys.* **135**, 114508.
- [Ward, 2012a] Ward, M., R. & Alexander, A., J. (2012). *Cryst. Growth Des.*, **12**, 4554 - 4561.
- [Ward, 2012b] Ward, M., R., McHugh, S. & Alexander, A., J. (2012). *Phys. Chem. Chem. Phys.*, 2012, **14**, 90 - 93.
- [Yang 2008] Yang, X., Wang, X. & Ching, C., B. (2008). *J. Chem. Eng. Data*, **53**, 1133 - 1137.

- [**Yennawar 2010**] Yennawar, N., Denev, S., Gopalan, V. & Yennawar, H. (2010). *Acta Cryst.* **F66**, 969 - 972.
- [**Yoshikawa 2006a**] Yoshikawa, H., Y., Hosokawa, Y. & Masuhara, H. (2006) *Jpn. J. Appl. Phys.* **45**, L23 - L26.
- [**Yoshikawa 2006b**] Yoshikawa, H., Y., Hosokawa, Y. & Masuhara, H. (2006). *Cryst. Growth Des.*, **6**, 302 – 305.
- [**Yoshikawa, 2009**] Yoshikawa, H., Y., Murai, R., Sugiyama, S., Sazaki, G., Kitatani, T., Takahashi, Y., Adachi, H., Matsumura, H., Murakami, S., Inoue, T., Takano, K. & Mori, Y. (2009). *J. Cryst. Growth*, **311**, 956 - 959.
- [**Yoshikawa, 2014**] Yoshikawa H., Y., Murai, R., Adachi H., Sugiyama, S., Maruyama, M., Takahashi, Y., Takano, K., Matsumura, H., Inoue, T., Murakami, S., Masuhara, H & Mori, Y. (2014). *Chem Soc Rev.*, DOI: 10.1039/c3cs60226e.
- [**Yu 2002**] Yu, L. Ng, K. (2002) *J. Pharm. Sci.*, **91**, 11, 2367-2375.
- [**Yuyama 2010**] Yuyama, K., Sugiyama, T. & Masuhara, H. (2010). *J. Phys. Chem. Lett.*, **1**, 1321 - 1325.
- [**Yuyama 2012**] Yuyama, K., Rungsimamon, T., Sugiyama, T. & Masuhara, H. (2012). *Cryst. Growth Des.*, **12**, 2427 - 2434.
- [**Zaccaro 2001**] Zaccaro, J., Matic, J., Myerson, A., S. & Garetz, B., A. (2001). *Cryst. Growth Des.*, **1**, 5 - 8.